# Electronic and Steric Effects on the Photoisomerization of Dimethylsulfoxide Complexes of Ru(II) Containing Picolinate

Daniel A. Lutterman,[†] Aaron A. Rachford,[‡,§] Jeffrey J. Rack,*[,‡] and Claudia Turro*[,†]

[†]Department of Chemistry, The Ohio State University, Columbus, Ohio 43210, United States, and [‡]Department of Chemistry and Biochemistry, Nanoscale and Quantum Phenomena Institute, Ohio University, Athens, Ohio 45701, United States

ABSTRACT Calculations were performed on $[Ru(tpy)(bpy)(dmso)]^{2+}$ (tpy = 2,2′:6′,2″-terpyridine; bpy = 2,2′-bipyridine, dmso = dimethylsulfoxide, **1**), *cis*-$[Ru(tpy)(Me-pic)(dmso)]^{+}$ (Me-pic = 6-methylpicolinate, **2**), *trans*-$[Ru(tpy)-(Me-pic)(dmso)]^{+}$ (**3**), and *trans*-$[Ru(tpy)(pic)(dmso)]^{+}$ (pic = picolinate, **4**) to gain an understanding of the differences in their photoisomerization behavior. The results do not support a promoting role for the σ^* ligand field (LF) states during excited-state S→O isomerization. Instead, the calculations show that the Ru−S bonding, the identity of the highest occupied molecular orbital, and steric interactions are important factors in dmso photoisomerization. Furthermore, the atom positioned trans to the S atom plays a critical role in promoting enhanced photoisomerizataion yields.
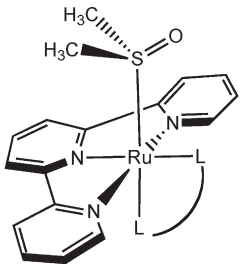
SECTION Molecular Structure, Quantum Chemistry, General Theory
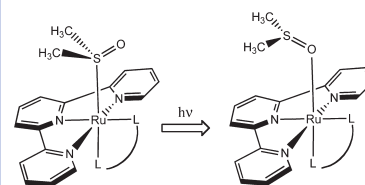
Photochromic compounds transduce photonic energy to potential energy to selectively break and form bonds within the excited state lifetime of the compound. The newly formed isomer or metastable state exhibits a distinct molecular and electronic structure from the ground state isomer. These reactions are of broad, general interest since they represent a light-driven thermodynamically uphill reaction, but they also provide a foundation for understanding the conversion of light to potential energy, a critical step in many photochemical processes. At present, there are a significant number of examples of both organic and inorganic complexes displaying photochromic behavior.[1−9]

We have recently investigated the S→O isomerization in a family of photochromic ruthenium polypyridine sulfoxide complexes by both computational and spectroscopic methods.[10−17] Our initial computational effort addressed the role of the ligand field (LF) states in complexes of the type $[Ru^{II}(tpy)(L)(dmso)]^{n+}$, where tpy is 2,2′:6′,2″-terpyridine, L is a variable bidentate ligand, dmso is dimethylsulfoxide, and n is 0, 1, or 2 dependent upon the charge of L.[18] The objective of the present study is to expand our density functional theory (DFT) computational efforts to better understand the isomerization mechanism as well as to provide a hypothesis for further investigation. Herein, we present our findings, which indicate that the extent of Ru−S bonding, the identity of the highest occupied molecular orbital (HOMO) and steric interactions are important factors in sulfoxide isomerization on ruthenium. Additionally, we find that the LF splitting energy is not a prominent factor in this reaction as might be predicted from many ruthenium polypyridine complexes.[19−36]

Photoisomerization from S-bonded to O-bonded dmso has been observed in $[Ru(tpy)(bpy)(dmso)]^{2+}$ (**1**; Figure 1;

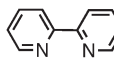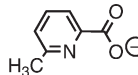**Figure 1.** Schematic representation of the molecular structures of $[Ru(tpy)(L)(dmso)]^{n+}$ complexes showing the structures of the ligand L with the numbering scheme.
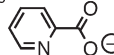
Complex	Abbreviation	Structure
1	bpy	
2 and 3	Me-pic	
4	pic	

bpy is 2,2′-bipyridine), with quantum yield ($\Phi_{S\rightarrow O}$) of 0.024 as listed in Table 1. The calculated MO diagram for **1** shown in Figure 2 is consistent with previous results.[18,37,38] A pictorial representation of the HOMO of **1** is shown in Figure 3a. This

Table 1. Photoisomerization Data for Complexes **1**−**4**

complex	L	$\Phi_{iso}{}^{a}$	Δ (eV)^{b}
1	bpy	0.024	5.45
2	*cis*-Me-pic	0.011	5.06
3	*trans*-Me-pic	0.79	5.39
4	*trans*-pic	0.25	5.39

^{a} From refs 14 and 15. ^{b} Δ is the energy difference between the metal-centered HOMO and the lowest energy Ru(dσ*) orbital.
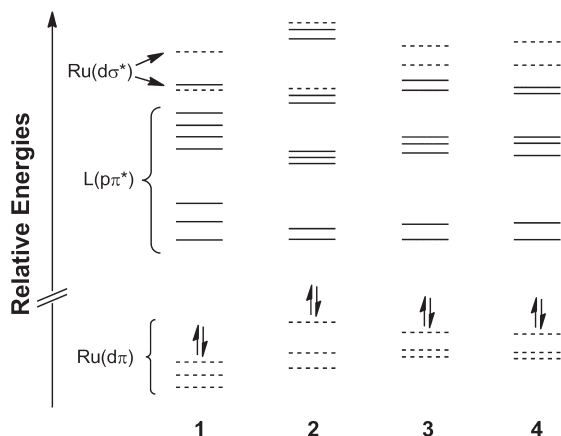

Figure 2. MO diagrams for **1**−**4** distinguishing orbitals with more metal character (---) from orbitals centered more on the ligands (——). The LUMOs were set at the same energy in all complexes.
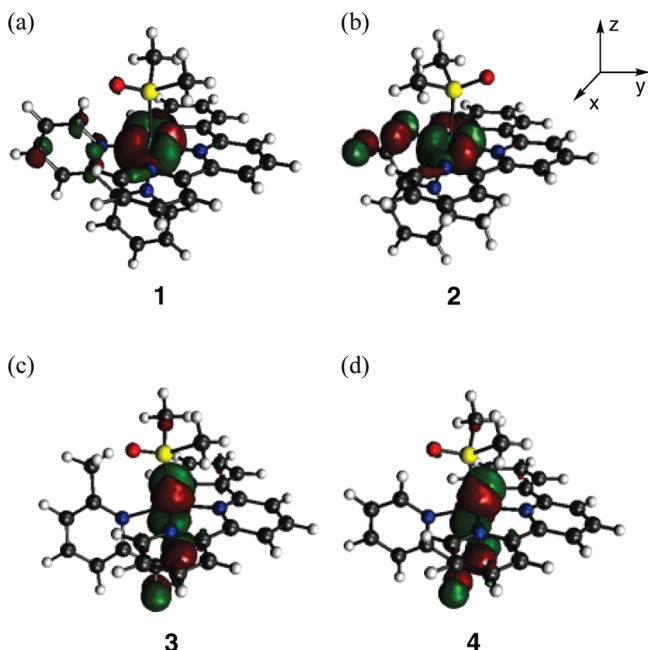

Figure 3. The HOMOs of complexes (a) **1**, (b) **2**, (c) **3**, and (d) **4** drawn with isovalue = 0.04.

MO is predominantly ruthenium dπ in character with modest contribution from the terpyridine and bipyridine rings and negligible contribution from the sulfoxide. Eight L(π*) MOs of **1** are centered on the tpy and bpy ligands, seven of which

Table 2. Metrical (Ru−S Bond Distance), Absorption ($\lambda_{max,abs}$) and Reduction Potential ($E_S{}^{o\prime}$ Ru$^{3+/2+}$) Data for Complexes **2**−**4**

complex	Ru−S (Å)	$\lambda_{max,abs}$ (nm)	$E_S{}^{o\prime}$ Ru$^{3+/2+}$ (V)
2	2.241(1)	447	+1.07
3	2.2564(6)	413	+1.30
4	2.2152(5)	419	+1.31

comprise the lowest unoccupied MOs (LUMOs). In these MO diagrams, we have chosen to place the lowest energy tpy(π*) orbital at the same energy, consistent with invariance of the first reduction potential of complexes **1**−**4**.[14,15] Two metal-centered unoccupied orbitals, Ru(dσ*), are found at higher energy than the tpy(π*) MOs (Figure 2), consistent with expectation.

As listed in Table 1, the photoisomerization quantum yield of *cis*-[Ru(tpy)(Me-pic)(dmso)]$^{+}$ (**2**, Me-pic is 6-methylpicolinate), $\Phi_{S\rightarrow O}$ = 0.011, is similar to that of **1** ($\Phi_{S\rightarrow O}$ = 0.024). Like **1**, the calculated MO diagram of **2** has a set of three metal-centered Ru(dπ) HOMOs and a set of tpy(π*) orbitals that comprise the manifold of LUMOs (Figure 2). The Ru(dσ*) set are higher in energy than the tpy(π*) set, exhibiting a Δ of 5.06 eV (40 796 cm^{-1}), where Δ represents the energy difference between the metal-centered HOMO and the lowest energy Ru(dσ*) orbital. The smaller value of Δ for **2** compared to that of **1**, 5.45 eV (43 957 cm^{-1}) is expected since the former has a π-donor ligand in the coordination sphere. In both **1** and **2** the highest occupied Ru(dπ) MOs are mostly metal centered, but in **2** there is a substantial contribution (11.6%) to the HOMO from the oxygen atoms of the Me-pic ligand (Figure 3b). The symmetry of the p$_x$ orbital of the oxygen atom matches that of the d$_{xy}$ orbital of the ruthenium atom and destabilizes the HOMO through π-bonding to this orbital as compared to the d$_{xz}$ and d$_{yz}$.

It is apparent in the MO diagrams of complexes **3** and **4** shown in Figure 2 that the dπ orbital manifold is stabilized relative to **2**, consistent with electrochemical measurements (Table 2). The electron density plots of the HOMOs for **3** and **4** are compared to those of **1** and **2** in Figure 3. It is interesting to note that the HOMO of **1** and **2** corresponds to the d$_{xy}$ orbital, whereas for **3** and **4** the HOMO can be ascribed to the d$_{xz}$ orbital of ruthenium. Moreover, as is shown in Figure 3, the ruthenium d$_{xz}$ orbital in **3** and **4** contains sizable sulfur character (1.1 and 0.8%, respectively), unlike those of **1** and **2** (0.1 and 0.2%, respectively). As expected for the presence of a π-donor ligand, the HOMO of **2**, **3**, and **4** each contain substantial oxygen character from the corresponding picolinate ligand, 11.6, 13.6, and 12.9%, respectively. However, for **3** and **4**, this interaction is along the z-axis, in a position *trans* to the sulfur atom. Indeed, the presence of the oxygen atom along the z-axis raises the energy of the d$_{xz}$ orbital making it the HOMO in **3** and **4**. The Δ values of **3** and **4** are both 5.39 eV (43 509 cm^{-1}), much larger than that of **2**, making the ^{3}LF dd state(s) in complexes **3** and **4** much less thermally accessible.

The $\Phi_{S\rightarrow O}$ values for **3** and **4** are 0.79 and 0.25, respectively, and are displayed in Table 1. The calculated value of Δ for **2** represents the smallest separation in the complexes **1**−**4**, but its quantum yield of isomerization is the lowest for

these complexes. This finding further suggests that the [3]LF dd state(s) are not involved in S→O photoisomerization, since it is expected that a decrease in Δ would make the [3]LF dd state(s) more thermally accessible. Furthermore, the quantum yield of S→O photoisomerization in **3** is 0.79, the largest value recorded for all of the studied Ru(II) dmso complexes, exhibits the largest Δ value among complexes **2−4**, and is similar to that of **1**. These observations are inconsistent with the involvement of the [3]LF dd states in S→O photoisomerization in these complexes.

Comparison of **2** with **3** and **4** allows for direct evaluation of the *trans*-effect in this photoisomerization. For complexes **3** and **4**, the HOMO has both Ru−S bonding and Ru−O antibonding character. Following metal-to-ligand charge transfer (MLCT) excitation, removal of electron density from the HOMO results in weakening of the Ru−S bond, with concomitant strengthening of the Ru−O bond. In **2**, excitation does not formally involve an orbital with sulfur character, and the Ru−O bond, although strengthened, is not *trans* to the dmso ligand. We speculate that oxidation via MLCT excitation of the d_{xz} orbital in **3** and **4** promotes S→O isomerization, consistent with the larger $\Phi_{S\rightarrow O}$ values. In another complex that features a large quantum yield ([Ru(bpy)$_2$(OSO)]$^+$, OSO is 2-methylsulfinylbenzoate, $\Phi_{S\rightarrow O} = 0.45$), the lowest energy MLCT transition was calculated to possess contributions from the d_{xz} and d_{yz} orbitals, both of which contain Ru−S bonding character.[39] Accordingly, excitation results in a weakening of the Ru−S bond, thus triggering isomerization or rapid and substantial reorganization away from the Franck−Condon state during excited state evolution. A result consistent with this interpretation was found in DFT computational studies of dmso (S→O) isomerization on pentaammineruthenium(III).[40]

Although **3** and **4** have nearly identical electronic structures as determined by our DFT calculations, the $\Phi_{S\rightarrow O}$ differ by more than a factor of 3. The origin of this effect may be found from an examination of the experimental data. The observed MLCT absorption maxima differ by just 6 nm (Table 2), the Ru$^{3+/2+}$ reduction potentials differ by 0.01 V, and the tpy$^{0/−}$ reduction potentials are identical. However, comparison of the molecular structures as determined by X-ray crystallography reveal some important differences (Table 2). For instance, the Ru−S bond distance for **3** is 2.2564(6) Å, which is significantly longer than that observed for **4**, 2.2152(5) Å. A similar contraction in the Ru−S bond length by 0.04 Å is observed in the calculated ground-state structure of **4** as compared to **3**. Furthermore, the angles defined by N$_{picolinate}$−Ru1−S1 are 106.43° and 97.44° in **3** and **4**, respectively. Also, the torsion angle defined by O$_{sulfoxide}$−S1−Ru1−N$_{picolinate}$ is larger for **3** (57.4°) than for **4** (51.7°). In aggregate, these data support the notion that the Me-pic ligand exerts a strong ground-state steric effect resulting in a longer, weaker Ru−S bond in **3** compared to **4**. Such a weaker bond is more easily broken upon excitation, possibly leading to a greater $\Phi_{S\rightarrow O}$ value in **3** compared to **4**. It should also be noted that the geometry in **2** does not suggest overcrowding from the unique bidentate ligand and exhibits a Ru−S bond distance of 2.241(1) Å and O$_{picolinate}$−Ru1−S1 angle of 89.9°, consistent with an ideal octahedral geometry and lower $\Phi_{S\rightarrow O}$ value, similar to that of **1**.

The calculations presented here show that the coordination environment about ruthenium determines the identity of the metal-centered HOMO. For **1** and **2**, the nitrogen atom positioned *trans* to the sulfur atom renders the ruthenium d_{xy} orbitial at highest energy, whereas for **3** and **4** the highest energy orbital is d_{xz} with non-negligible Ru−S bonding character due to the *trans* disposition of the oxygen atom relative to the sulfur atom. Accordingly, removal of an electron from this orbital in the MLCT excited state promotes significantly greater isomerization quantum yields in **3** and **4** relative to **1** and **2**. The presence of the methyl group on the unique bidentate ligand in **3** further enhances the phototriggered S→O isomerization quantum yield. The findings now permit us to design additional complexes with improved photochemistry.

EXPERIMENTAL SECTION

All calculations were performed using the Gaussian 03 (G03) program package,[41] with the Becke three-parameter hybrid exchange and the Lee−Yang−Parr correlation functionals (B3LYP).[42−44] The 6-31G* basis set was used for H, C, N, O, and S (using five pure d functions),[45] along with the Stuttgart/Dresden (SDD) energy-consistent pseudopotentials for Ru.[46,47] All geometry optimizations were performed in C_1 symmetry with subsequent vibrational frequency analysis to confirm that each stationary point was a minimum on the potential energy surface. Orbital analysis was computed using Molekel 4.3.win32.[48]

The percentage of atomic character in some of the occupied (canonical) MOs in the complexes was calculated from a full population analysis, using eq 1:

$$\%AC_j = \left[\sum_i (\phi_{i,j})^2 / \sum_i \sum_j (\phi_{i,j})^2\right] \times 100 \qquad (1)$$

where $\%AC_j$ represents the percent atomic character of atom j to the MO of interest and $\phi_{i,j}$ is the eigenvalue of atomic orbital i of atom j that contributes to that MO. This calculation was performed on the three highest occupied orbitals of each complex.

SUPPORTING INFORMATION AVAILABLE
Complete reference 41 and Cartesian coordinates for **1−4**. This material is available free of charge via the Internet at http://pubs.acs.org.

AUTHOR INFORMATION

Corresponding Author:
*To whom correspondence should be addressed. E-mail: turro@chemistry.ohio-state.edu (C.T.); rackj@ohio.edu (J.J.R.).

Present Addresses:
§ Present address: The Dow Chemical Company, Analytical Sciences, 1897 Building, Midland, MI 48667, USA.

REFERENCES

(1) Rack, J. J. Electron Transfer Triggered Sulfoxide Isomerization in Ruthenium and Osmium Complexes. *Coord. Chem. Rev.* **2009**, *253*, 78–85.

(2) McClure, B. A.; Rack, J. J. Isomerization in Photochromic Ruthenium Sulfoxide Complexes. *Eur. J. Inorg. Chem.* **2010**, 3895–3904.

(3) Browne, W. R.; Feringa, B. L. Light Switching of Molecules on Surfaces. *Annu. Rev. Phys. Chem.* **2009**, *60*, 407–428.

(4) Irie, M. Diarylethenes for Memories and Switches. *Chem. Rev.* **2000**, *100*, 1685–1716.

(5) Kume, S.; Nishihara, H. Photochrome-Coupled Metal Complexes: Molecular Processing of Photon Stimuli. *Dalton Trans.* **2008**, 3260–3271.

(6) Wang, M. S.; Xu, G.; Zhang, Z. J.; Guo, G.-C. Inorganic–Organic Hybrid Photochromic Materials. *Chem. Commun.* **2010**, 361–376.

(7) Yildiz, I.; Deniz, E.; Raymo, F. M. Fluorescence Modulation with Photochromic Switches in Nanostructured Constructs. *Chem. Soc. Rev.* **2009**, 1859–1867.

(8) Wigglesworth, T. J.; Myles, A. J.; Branda, N. R. High Content Photochromic Polymers Based on Dithienylethenes. *Eur. J. Org. Chem.* **2005**, 1233–1238.

(9) To, T. T.; Heilweil, E. J.; Duke, C. B.; Ruddick, K. R.; Webster, C. E.; Burkey, T. J. Development of Ultrafast Photochromic Organometallics and Photoinduced Linkage Isomerization of Arene Chromium Carbonyl Derivatives. *J. Phys. Chem. A* **2009**, *113*, 2666–2676.

(10) Smith, M. K.; Gibson, J. A.; Young, C. G.; Broomhead, J. A.; Junk, P. C.; Keene, F. R. Photoinduced Ligand Isomerization in Dimethyl Sulfoxide Complexes of Ruthenium(II). *Eur. J. Inorg. Chem.* **2000**, 1365–1370.

(11) Rack, J. J.; Winkler, J. R.; Gray, H. B. Phototriggered Ru(II)-Dimethylsulfoxide Linkage Isomerization in Crystals and Films. *J. Am. Chem. Soc.* **2001**, *123*, 2432–2433.

(12) Rack, J. J.; Mockus, N. V. Room-Temperature Photochromism in *cis*- and *trans*-[Ru(bpy)$_2$(dmso)$_2$]$^{2+}$. *Inorg. Chem.* **2003**, *42*, 5792–5794.

(13) Rack, J. J.; Rachford, A. A.; Shelker, A. M. Turning-Off Phototriggered Linkage Isomerizations in Ruthenium Dimethylsulfoxide Complexes. *Inorg. Chem.* **2003**, *42*, 7357–7359.

(14) Rachford, A. A.; Petersen, J. L.; Rack, J. J. Designing Molecular Bistability in Ruthenium Dimethylsulfoxide Complexes. *Inorg. Chem.* **2005**, *44*, 8065–8075.

(15) Rachford, A. A.; Petersen, J. L.; Rack, J. J. Efficient Energy Conversion in Photochromic Ruthenium DMSO Complexes. *Inorg. Chem.* **2006**, *45*, 5953–5960.

(16) Rachford, A. A.; Rack, J. J. Picosecond Isomerization in Photochromic Ruthenium DMSO Complexes. *J. Am. Chem. Soc.* **2006**, *128*, 14318–14324.

(17) Butcher, D. P., Jr.; Rachford, A. A.; Petersen, J. L.; Rack, J. J. Phototriggered S→O Isomerization of a Ruthenium-Bound Chelating Sulfoxide. *Inorg. Chem.* **2006**, *45*, 9178–9180.

(18) Lutterman, D. A.; Rachford, A. A.; Rack, J. J.; Turro, C. Theoretical Insight on the S→O Bound Photoisomerization of DMSO Complexes of Ru(II). *J. Phys. Chem. A* **2009**, *113*, 11002–11006.

(19) Kober, E. M.; Meyer, T. J. Concerning the Absorption Spectra of the Ions M(bpy)$_3$$^{2+}$ (M = Fe, Ru, Os; bpy = 2,2'-Bipyridine). *Inorg. Chem.* **1982**, *21*, 3967–3977.

(20) Caspar, J. V.; Meyer, T. J. Photochemistry of Ru(bpy)$_3$$^{2+}$. Solvent Effects. *J. Am. Chem. Soc.* **1983**, *105*, 5583–5590.

(21) Caspar, J. V.; Meyer, T. J. Photochemistry of MLCT Excited-States. Effect of Nonchromophoric Ligand Variations on Photophysical Properties in the Series *cis*-Ru(bpy)$_2$L$_2$$^{2+}$. *Inorg. Chem.* **1983**, *22*, 2444–2453.

(22) Kober, E. M.; Meyer, T. J. An Electronic Structural Model for the Emitting MLCT Excited-States of Ru(bpy)$_3$$^{2+}$ and Os(bpy)$_3$$^{2+}$. *Inorg. Chem.* **1984**, *23*, 3877–3886.

(23) Juris, A.; Balzani, V.; Barigelletti, F.; Campagna, S.; Belser, P.; Von Zelewsky, A. Ru(II) Polypyridine Complexes: Photophysics, Photochemistry, Electrochemistry, and Chemiluminescence. *Coord. Chem. Rev.* **1988**, *84*, 88–277.

(24) Lumpkin, R. S.; Kober, E. M.; Worl, L. A.; Murtaza, Z.; Meyer, T. J. Metal-to-Ligand Charge Transfer (MLCT) Photochemistry. Experimental Evidence for the Participation of a Higher Lying MLCT State in Polypyridyl Complexes Ruthenium(II) and Osmium(II). *J. Phys. Chem.* **1990**, *94*, 239–243.

(25) Barigelletti, F.; Flamigni, L.; Balzani, V.; Collin, J.-P.; Sauvage, J.-P.; Sour, A.; Constable, E. C.; Thompson, A. M. W. C. Intramolecular Energy Transfer through Phenyl Bridges in Rod-like Dinuclear Ru(II)/Os(II) Terpyridine-type Complexes. *Coord. Chem. Rev.* **1994**, *132*, 209–214.

(26) Damrauer, N. H.; Cerullo, G.; Yeh, A.; Boussie, T. R.; Shank, C. V.; McCusker, J. K. Femtosecond Dynamics of Excited-State Evolution in Ru(bpy)$_3$$^{2+}$. *Science* **1997**, *275*, 54–87.

(27) Baba, A. I.; Shaw, J. R.; Simon, J. A.; Thummel, R. P.; Schmehl, R. H. The Photophysical Behavior of d^6 Complexes having Nearly Isoenergetic MLCT and Ligand Localized Excited States. *Coord. Chem. Rev.* **1998**, *171*, 43–59.

(28) Damrauer, N. H.; McCusker, J. K. Ultrafast Dynamics in the Metal-to-Ligand Charge Transfer Excited-State Evolution of [Ru(4,4'-diphenyl-2,2'-bipyridine)$_3$]$^{2+}$. *J. Phys. Chem. A* **1999**, *103*, 8440–8446.

(29) McCusker, J. K. Femtosecond Absorption Spectroscopy of Transition Metal Charge-Transfer Complexes. *Acc. Chem. Res.* **2003**, *36*, 876–887.

(30) Wang, X.-Y.; Guerzo, A. D.; Schmehl, R. H. Photophysical Behavior of Transition Metal Complexes Having Interacting Ligand Localized and Metal-to-Ligand Charge-Transfer States. *J. Photochem. Photobiol. C* **2004**, *5*, 55–77.

(31) Baranoff, E.; Collin, J.-P.; Flamigni, L.; Sauvage, J.-P. From Ruthenium(II) to Iridium(III): 15 Years of Triads Based on bis-Terpyridine Complexes. *Chem. Soc. Rev.* **2004**, *33*, 147–155.

(32) Baitalik, S.; Wang, X.-Y.; Schmehl, R. H. A Trimetallic Mixed Ru(II)/Fe(II) Terpyridyl Complex with a Long-Lived Excited State in Solution at Room Temperature. *J. Am. Chem. Soc.* **2004**, *126*, 16304–16305.

(33) Abrahamsson, M.; Jager, M.; Osterman, T.; Eriksson, L.; Persson, P.; Becker, H.-C.; Johansson, O.; Hammarstrom, L. A 3 μs Room Temperature Excited State Lifetime of a bistridentate Ru(II) Polypyridine Complex for Rod-like Molecular Arrays. *J. Am. Chem. Soc.* **2006**, *128*, 12616–12617.

(34) Kirchhoff, J. R.; McMillin, D. R.; Marnot, P. A.; Sauvage, J.-P. Photochemistry and Photophysics of bis(terpyridyl) Complexes of Ru(II) in Fluid Solution. Evidence for the Formation of an η^2-Diphenylterpyridine Complex. *J. Am. Chem. Soc.* **1985**, *107*, 1138–1141.

(35) Suen, H.-F.; Wilson, S. W.; Pomerantz, M.; Walsh, J. L. Photosubstitution Reactions of Terpyridine Complexes of Ruthenium(II). *Inorg. Chem.* **1989**, *28*, 786–791.

(36) Hecker, C. R.; Fanwick, P. E.; McMillin, D. R. Evidence for Dissociative Photosubstitution Reactions of [Ru(trpy)(bpy)(NCCH$_3$)]$^{2+}$. Crystal and Molecular Structure of [Ru(trpy)(bpy)(py)](PF$_6$)$_2$·(CH$_3$)$_2$CO. *Inorg. Chem.* **1991**, *30*, 659–666.

(37) Ciofini, I; Daul, C. A.; Adamo, C. Phototriggered Linkage Isomerization in Ruthenium Dimethylsulfoxyde Complexes: Insight from Theory. *J. Phys. Chem. A* **2003**, *107*, 11182.

(38) Borg, O. A.; Godinho, S. S. M. C.; Lundqvist, M. J.; Lunell, S.; Persson, P Computational Study of the Lowest Triplet State of Ruthenium Polypyridyl Complexes Used in Artificial Photosynthesis. *J. Phys. Chem. A.* **2008**, *112*, 4470–4476.

(39) McClure, B. A.; Mockus, N. V.; Butcher, D. P., Jr.; Lutterman, D. A.; Turro, C.; Petersen, J. L.; Rack, J. J. Photochromic Ruthenium Sulfoxides Complexes: Evidence for Isomerization Through a Conical Intersection. *Inorg. Chem.* **2009,** *48*, 8084–8091.

(40) Panina, N. S.; Calligaris, M. Density Functional Study of Linkage Isomerism in Dimethyl Sulfoxide Ru(III) and Rh(III) Complexes. *Inorg. Chim. Acta* **2002,** *334*, 165–171.

(41) Frisch, M. J.; Trucks, G. W.; Schlegel, H. B.; Scuseria, G. E.; Robb, M. A.; Cheeseman, J. R.; Montgomery, J. A., Jr.; Vreven, T.; Kudin, K. N.; Burant, J. C.; et al. *Gaussian 03*, revision C.02; Gaussian Inc.; Wallingford, CT, 2004.

(42) Becke, A. D. Density Functional Thermochemistry. 3. The Role of Exact Exchange. *J. Chem. Phys.* **1993,** *98*, 5648–5652.

(43) Becke, A. D. Density-Functional Exchange-Energy Approximation with Correct Asymptotic Behavior. *Phys. Rev. A: Gen. Phys.* **1988,** *38*, 3098–3100.

(44) Lee, C.; Yang, W.; Parr, R. G. Development of the Colle− Salvetti Correlation-Energy Formula into a Functional of the Electron Density. *Phys. Rev. B: Condens. Matter Mater. Phys.* **1988,** *37*, 785–789.

(45) Hehre, W. J.; Radom, L.; Schleyer, P. V. R.; Pople, J. A. *Ab Initio Molecular Orbital Theory*; John Wiley & Sons: New York, 1986.

(46) Dolg, M.; Stoll, H.; Preuss, H. A Combination of Quasi-Relativistic Pseudopotential and Ligand Field Calculations for Lanthanoid Compounds. *Theor. Chim. Acta* **1993,** *85*, 441–450.

(47) Wedig, U.; Dolg, M.; Stoll, H. *Quantum Chemistry: The Challenge of Transition Metals and Coordination Chemistry*; Veilard, A., Ed.; D. Reidel Publishing Company: Dordrecht, The Netherlands, 1986.

(48) Flükiger, P.; Lüthi, H. P.; Portmann, S.; Weber, J. *MOLEKEL 4.3*; Swiss Center for Scientific Computing: Manno, Switzerland, 2000; www.cscs.ch/molekel.